A ROBOTIC SYSTEM FOR *IN SITU* HYDROPOWER TURBINE HARD COATING

Renan S. Freitas*, Estevão F. Ferrão*, Gabriel Alcantara C. S.*, Eduardo Elael M. S.*, Ramon R. Costa*

**Department of Electrical Engineering, COPPE UFRJ, Rio de Janeiro, Brasil.*

Emails: `renan028@gmail.com, ef.ferrao@mecanica.coppe.ufrj.br, alcantara@poli.ufrj.br, elael2@gmail.com, ramonrcosta@gmail.com`

Abstract— Hard coating of hydropower turbine's blades increase power generation efficiency and system's life cycle. Currently, blade coating is an *ex situ* process limited to unassembled turbines. EMMA is a robotic solution for *in situ* hard coating maintenance. The system operates in the confined turbine's environment, and complies the hard coating process requirements. The proposed system is composed of modular and customized rails, a robotic manipulator, and sensors for control, localization and mapping. The simulations and field tests validate the concepts considered so far and rise several challenges for future works.

Keywords— Hard coating, manipulator, robotics, robot calibration, rail system, hydropower

Resumo— O processo de metalização das pás de turbinas hidrelétricas aumenta a eficiência da geração de energia, e sua vida útil. Atualmente, o revestimento das pás é um processo realizado fora do ambiente da turbina. EMMA é uma solução robótica para manutenção *in situ* por metalização de pás de turbinas hidrelétricas. O sistema opera no espaço confinado da turbina, e cumpre com as restrições do processo de metalização. O sistema é composto por trilhos modulares e customizados, um manipulador industrial robótico, e sensores para controle, mapeamento e localização. As simulações e testes de campo validam os conceitos considerados e levantam novos desafios para trabalhos futuros.

Keywords— Metalização, manipulador robótico, robótica, calibração, sistemas em trilhos, hidrelétrica

1 Introduction

Hydropower has an important share in the global electricity production, and will continue to be a major source of renewable power-generation[1]. In hydropower generating plants, the average maintenance cost is 2% of the investment cost per kW, and, typically, the large mechanical components, as turbines, must be maintained and replaced every 25 years. The cavitation and abrasion phenomena on the turbine's blades have become a concern, as the erosion can lead to water flow instability, excessive vibrations and turbine efficiency reduction (Goldemberg and Lucon, 2007). Hard coating techniques by thermal aspersion are used to greatly increase the life cycle of runner's blades (Krella, 2011).

In the specific case of Brazil, hydropower is the largest power-generation source. To support future economic growth, Brazil has invested in additional large hydroelectric facilities, for instance, the 14 GW Belo Monte along the Xingu River[2], and Jirau dam (Fig. 1) along the Madeira river. At the latter, the high concentration of suspended particles carried by the river intensifies the abrasion phenomena, thus regular maintenance is needed. Currently, blade coating maintenance in these large facilities is performed before turbine assembling by a large-sized robotic manipulator.

Repair maintenance, as grinding and welding, can be done manually in the turbine's environment, but the hard coating procedure requires a robotic system due to high precision, speed, and the usage of hazardous substances. There are several difficulties encountered when attempting to robotize *in situ* maintenance, as accessibility, system placement and calibration. A few robotic systems have been investigated to perform *in situ* repair of turbine runners, as it could greatly improve efficiency and safety, but none has been used for the hard coating operation. Some examples found in the literature are:

Figure 1: Jirau's hydropower turbine.

- The Roboturb (Bonacorso et al., 2006) and the Scompi (Bibuli et al., 2007) are robotic systems to perform erosion inspection and welding on damaged runner's blades. They move on a flexible rail, which may be shaped and then fixed to the blade surface.
- *The Climber*[3] is an intervention robot for

[1]International Energy Agency (2010), http://www.iea.org/.

[2]Energy Information Administration (2014), https://www.eia.gov/.

[3]International Climbing Machines (2013), http://www.icm.cc/.

wind and hydroelectric turbines, to perform coating removal, surface cleaning and coating application. It is a climbing robot with pneumatic adhesion and locomotion by tracks.

In this paper, we present a general overview of a robotic system called EMMA, and a detailed description of the mechanics, the manipulator, and calibration. The system performs *in situ* hydropower runner's blade hard coating.

2 The hard coating process

Hydropower runner's blades are typically eroded by cavitation and abrasion phenomena, resulting in hydraulic profile deformation, thus efficiency reduction. The High Velocity Oxygen Fuel (HVOF) coating is a preventive solution for erosion, and creates a lamellar structure.

The HVOF is a 2000 hp power process which consists of spraying coating particles by an 8 kg spray gun, through a flame with mixed gases. To achieve the best coating layer, the spray gun should be at a fixed 210 mm to 240 mm distance, and $90° \pm 30°$ angle, in respect to the metallic surface plane of the blade; and the gun should move at 40 m/min speed along the path (Li and Wang, 2002). Besides, for a regular coating cover, the trajectory is 3 mm spaced horizontal lines crossing the blade's surface (coating step), which requires great positional accuracy of the robot. The common solution which meets the requirements for *ex situ* HVOF coating is a robotic manipulator with a blade-sized workspace in a fixed position.

3 The problem

The problem is to design a robotic system for *in situ* hydropower runner's blades. Accessibility is a major problem: the robot must be brought to the turbine through a hatch; and it must operate in the confined, curved, slippery and harsh environment of the turbine. Besides, there are several control and calibration problems, as trajectory planning, and robot localization.

The mechanical challenges are robot locomotion, base stiffness, and fixation. The robot should be transported and positioned in turbine's environment, as the access is generally far from the runner's blade. The stiffness is required for the hard coating process, since a base's vibrations are propagated to the manipulator's end-effector with high amplitudes, compromising the coating quality.

Regarding calibration, the relative position between the manipulator and the blade is not fixed. The system calibration consists in the identification of the manipulator and blade, and their pose estimation in respect to the turbine interior. Due to the environment's light conditions, 3D laser sensing technology should be used to map the topography of the blade, and the robotic system.

Large-sized manipulators are not suitable for *in situ* operations, due to the accessibility, and conventional compact manipulators do not have the required work envelope or payload for the task. Therefore, customized or mid-sized manipulators should be investigated by kinematics and dynamics simulations. Besides, the modeling of curvilinear space, the automatically trajectory generation, and the robot position and velocity control comprise the robot control strategy.

4 Solution

EMMA robotic technology is described in this section. The following system's elements will be presented: the robotic manipulator; the customized modular base; and the robot calibration.

4.1 Robotic Manipulator

The HVOF coating requirements and environment constraints demand a mid-sized robotic manipulator (Sec. 2). A survey was conducted to determine the most adaptable off-the-shelf manipulator for the application. Overall simulations and analysis were performed using the OpenRave (Diankov and Kuffner, 2008), an environment for simulating motion planning algorithms for robotics. There are several tools for dynamics simulation of robots: Gazebo, V-Rep, Webots, and others. OpenRave was selected because of its integral design for real-time control and execution monitoring, the core functionality for kinematics operations and physics simulations, and the ROS support, simplifying future software integration.

The simulations were performed to analyze the manipulator's work envelope in the turbine, the required positions for full blade coating, the manipulator's efforts (torque estimation), and to investigate possible collisions with mechanical parts. The simulations steps are runner's blade discretization, manipulator's base position computations for full cover, and robotic manipulator's kinematics and dynamics.

The blade's surface discretization is an uniform sampling of the blade, determining the manipulator's end-effector directions. The current approach is to take the bounding box of the blade and sample its surface uniformly. Once the surface of the box is sampled, the intersection of the blade and a ray originating from each point going inward is taken. The normal of the blade's surface from each of these intersection points is taken to be the end-effector direction. The resulting samples are translated 230 mm in respect with their normal vectors, and collisions with the environment are checked.

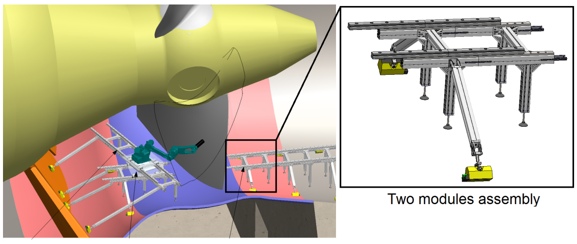

Figure 2: Customized base: primary and secondary rails.

Manipulator's base position computations are to uniformly sample the turbine's confined space and to calculate the minimum required positions to process all the blade's samples, considering angle and distance tolerances of the process. It is a brute force search: for each position, inverse kinematics are computed to determine the manipulator's joint parameters that provide the desired positions and orientations of the end-effector.

The kinematic approach described above is not enough to ensure that the robot will reach the samples. Maximum accelerations and torques should be investigated and compared to the manipulator's specifications. To do this, we employ the well know relation: $\tau = M(q)\ddot{q} + C(q,\dot{q})\dot{q} + G(q)$ (Sciavicco and Siciliano, 2000), where τ is the joints' torques, M is the matrix of moments of inertia estimated by manipulator's CAD model, q is the joints' angles, C is the Coriolis matrix, and G is the gravity vector. The angular accelerations are derived by differential kinematics: $\ddot{q} = J^{\dagger}(\ddot{x} - \dot{q}^T H \dot{q})$, where H is the Hessian matrix (Hourtash, 2005), $\ddot{x}$ is the linear accelerations, and $J^{\dagger}$ is the Jacobian matrix pseudoinverse. Therefore, torques can be analytically estimated by the inverse dynamics in OpenRave.

4.2 Mechanical system

EMMA's mechanical system is non-actuated rails for manipulator's base transportation, positioning and fixation. It comprises two rails, forming two prismatic joints (P-P). The first rail is parallel to the turbine axis, and it is responsible for the transportation of the manipulator from hatch to close to the blade. The secondary rail is assembled from the first by a rotational joint (R), which allows to position the upper rail parallel to the blade's surface.

The hatch limits the size of the rail in terms of weight and geometry, thus a modular concept was adopted, such that the small modular parts can be easily and manually assembled inside the turbine. Each module contains all the necessary components to support, transport and position the manipulator along it. Thus, the modules can be simply assembled in sequence to increase the overall length of the prismatic joint.

A two parallel profiled rail system with a four carriage setup[4] was adopted. This configuration creates a balanced force couple, eliminating the reaction moments in each carriage. The frame structure is formed by aluminum profile, since it is lightweight, corrosion resistant, geometrically flexible, and modular (easy rail reconfiguration by changing few parts or adding anchor arms).

The resulting frame structure is slender and lightweight, demanding careful dynamic analysis of its integrity and stiffness. A Finite Element Analysis (FEA) was performed to evaluate the stresses, strains and forces along the structure. FEA is also used to specify the frame components, such as the profile's size, and anchors quantity, dimensions, directions, and attachment points.

Since the draft tube and runner area are curved and sloped, properly fixing the mechanical base is a major challenge in EMMA. The draft tube is composed of a ferromagnetic steel material, hence magnetic fixtures is solution for base attachment without environment modifications, as welding.

4.3 Calibration

The calibration process was divided in two different approaches depending on the element to be localized and its caracteristics. The possibility to attach or install markers in known positions dictated the strategies to be chosen, therefore the calibration is separeted in the pose estimation of the robot and of the blade, as follows.

The attachment of markers on the robotic manipulator can be performed with high precision and repeatability, thus reflective spheres were chosen as reference points in the process of robot localization. These spheres are identified inside the point cloud by the 3D Hough Transform method (Camurri et al., 2014). The 3D Hough Transform, as the 2D Hough Transform, is the search of an object on the (discretized) parametric space. A sphere has four parameters: three for the position of its center, and one for its radius. For each point on the point cloud, it is assigned a collection of voxels on the discretized parametric space, corresponding to the possible spheres passing through that point. As in a voting process, the voxels with the greatest number of points assigned to define the parameters of the most probable spheres. There might be computational issues depending on the size of the parameter space, but it can be mitigated by exploiting previous knowledge regarding the expected radius and viable region for the robot inside the enviroment. Further improvements can be achieved through the use of the normal vector at each point, exploiting the

[4] Profile Rail Guides LLT: Mounting maintenance and repair instructions, SKF Group.

fact that the center of the sphere is in the direction of the normal, thus reducing the number of assigned voxels per point and in consequence the computational effort.

Fixing any marker on the blade would require its own calibration to ensure a consistent reference point, thus the pose estimation of the blade must rely only on the intrinsec properties of its surface geometry. The information must be extracted from the point cloud (the scene) provided by the 3D laser sensor and compared to a reference model previously stored. The characteristics of the point clouds are represented by local descriptors, i.e., each interest point on the blade is associated with a piece of information about its local neighborhood. Given the sets of features from the model and the scence, it is possible to determine the correspondence between their descriptors. If enough correspondences are found in the scene, above a threshold, the blade is identified and the position can be determined (Tombari and Di Stefano, 2010).

As the blade is a large and smooth surface, the neighborhood of each point may introduce similiar information, creating ambiguous descriptors that degrade the matching perfomance, thus it is fundamental to wisely pick the interest points. The ambiguous descriptors provide information about perpendicular translation to the supporting plane, and the two rotations associated with it, thus no information about the other DOFs, making the alignment to "slide" from the correct transformation. Therefore, the interest points were sampled to diversify the normal vectors' directions (Rusinkiewicz and Levoy, 2001), allowing to reduction of the number of samples to have a descriptor associated, when compared to a uniform sampling, and maintaning the computational cost low.

Once the descriptors were estimated, the correspondences are determined if the euclidean distance between a descriptor in the scene and in the model is lower than a threshold. Each correspondence vote for a specific pose and scale factor in the Hough space. After an instance of the model is found, it is performed the Iterative Closest Point (ICP) matching with the full resolution point clouds to realize a fine alignment and compensate any discrepancy introduced by the sampling. With the position of the blade and the manipulator in respect to a common coordinate system, i.e., the origin of the laser sensor, it is possible to determine the transformation between them and this information can be fed to the trajectory and coverage algorithms. It is important to note that in every step of the operation, in which either the manipulator base or the blade are moved, there is the need to recalibrate the system.

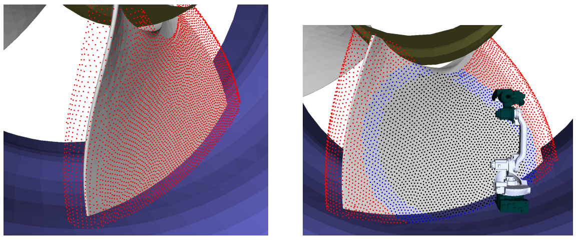

(a) Blade discretization (b) Manipulator workspace

Figure 3: Blade discretization and manipulator workspace for a fixed position.

5 Results

Simulations and experimental tests at Jirau's facility were performed to verify the proposed concepts. The results are divided according to the EMMA system's elements introduced in Sec. 4.

5.1 Robotic manipulator analysis

As stated in Subsec. 4.1, simulations for the robotic manipulator were implemented with OpenRave, and consist of the following steps: blade's surface discretization; base position computation; kinematics and dynamics.

A survey of off-the-shelf manipulators was conducted for Jirau's turbine. Regarding the runner's blade dimension, among the analyzed mid-sized robotic manipulators, the Yaskawa Motoman MH12 robot was chosen due to its satisfactory workspace, and versatility. Blade discretization is performed in a Jirau runner's blade CAD model, Fig. 3(a) shows the blade's samples, and Fig. 3(b) shows the manipulator workspace, where black dots are coated points and blue dots are coated points with the angle tolerance. Thus it is possible to create a coating strategy and to select the simplest base positions. The result is the minimum required positions for the robotic manipulator's base.

Comparing estimated torques with the technical specifications, dynamic simulations' results showed that the robotic manipulator should be placed at, at least, 1400 mm distance from the blade's surface plane. Placing the robot nearer would enhance the robotic manipulator's workspace, but it would increase also the torques.

Despite being able to coat approximately 50% of the blade on a fixed position, kinematic and dynamic analysis show that the MH12 robot cannot fully cover it vertically or horizontally, demanding extra 2-DOF along the blade's surface. The base position computations reveal that the blade's top extremities require a specific base position, reachable with a primary rail between the blades. Therefore, the MH12 robot will require at least four positions along the blade and one position on a primary rail, between blades.

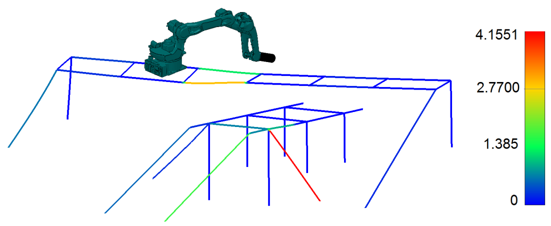

Figure 4: Von Mises's stress result.

5.2 *Mechanical system analysis*

In the specific case of Jirau, the secondary rail is customized with a third prismatic joint for height adjustment of the robotic manipulator. The primary and secondary rails with extra DOF guarantee the full coating, as they allow the robotic manipulator movement in the confined space by a 4-DOF base, PRPP joints.

The FEA of the base verifies the Von Mises stress and the displacements along the structure's slender members. The stress analysis determines the integrity of the base due to the maximum loads of the robotic manipulator. The displacements determine if the structure provides a rigid base for the robotic manipulator. According to the hard coating requirements, displacements of the order of millimeters are not allowable in the elastic region of the material.

The FEA solver was the Nastran In-CAD® with SolidWorks®. Model's elements are 1-D *bar line elements* with a global mesh's size of 25 mm. The material's properties are: density 2700 kg/m^3; Young modulus 70 GPa; Poisson's ratio 0.34; and Yield strength 200 MPa. Boundary conditions are three translational constraints for the anchors and a vertical constraint to the feet. The rotational joint is modeled as a rigid connector between the rails, such as the robot's base with respect to the second rail. The robotic manipulator's maximum dynamic forces and moments are applied, as static loads, to the point that represents the origin of the robot's base.

The maximum Von Mises stress was 4.16 MPa (Fig. 4), which gives a factor of safety of 34.6. It was found for a particular case where the robotic manipulator is in the secondary rail, 800 mm from the rotational joint. The displacement of the structure causes a maximum translation of 0.47 mm and a angular deflection of 0.0149° in respect to robotic manipulator base's coordinate system.

The field tests conducted in the draft tube for the magnetic fixtures, at different equipment's orientations and places, confirmed the manufacturer's payload capacity. As the maximum tractive reaction force obtained in FEA simulations was 956 kgf, it was chosen a magnetic fixture with 1200 kgf payload capacity.

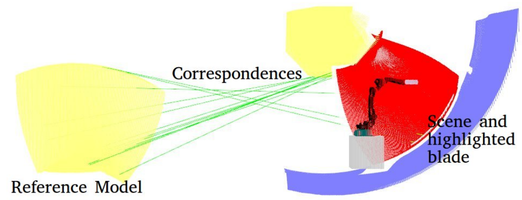

Figure 5: Blade reference model localized in the turbine environment with occlusions.

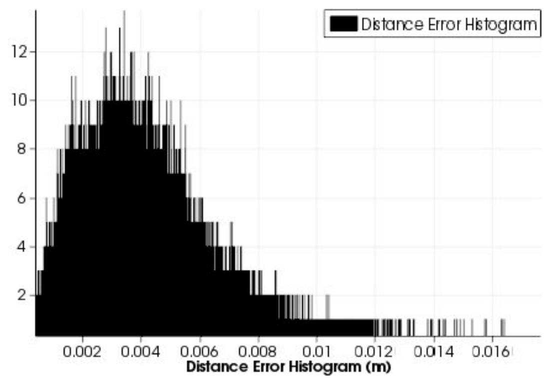

Figure 6: Histogram of the error (meters) between the model and reference scene point to point.

5.3 *Calibration analysis*

To test the calibration algorithm for the blades, the turbine environment and the robotic manipulator were simulated with help of the toolbox Blensor (Gschwandtner et al., 2011) and based on the technical drawings from the powerplant. The blade model, however, was acquired in a field test by a 3D laser scanner for a better representantion of the actual hidraulic profile.

The laser sensor was modeled following manufacturer's technical specifications, and different scenes were generated for several sensor positions. The algorithm is able to localize the blade in respect to the sensor's coordinate system, even in occlusion generated by the presence of the robotic manipulator. In Fig. 5, it can be seen the correspondeces between the reference model and the scene, or the turbine environment, and also the correctly localized blade instance highlighted in red.

The Fig. 6 exemplifies the error or distance distribution to the closest point from the scene to each point of the model. The mean distance between each swipe of the laser scan is 9 mm and the RMS error is 4 mm, which is consistent as the half of the resolution of the point clouds.

Similar procedure was followed to recreate a scene with four reference spheres (supposedly attached to the robot). The 3D Hough Method was able to locate all spheres' centers within a 5mm error (fig. 7).

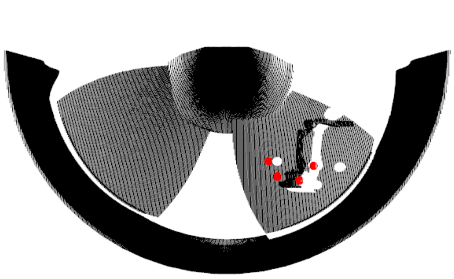

Figure 7: Points recognized as belonging to the four spheres (in red).

6 Conclusion and future work

In this paper, we presented the concept solution and detailed some aspects of the EMMA robotic system, for the problem of *in situ* hard coating system of hydropower turbine. All the robotic systems seen so far were developed for repairing by wielding or inspection applications, but the challenging requirements and constraints of the *in situ* HVOF coating procedure were not yet considered.

Climbers and robotic systems on rails attached to the blade were investigated as general solutions. However, these systems typically have small payloads and low speed, which do not meet the process' requirements. The design of these systems would be very complex, due to the blade's temperature variation, and the locomotion and adhesion mechanisms. The proposed system is simpler, similar to the *ex situ* solution, and the modular concept offers flexibility to logistics.

EMMA methodology and some elements of the system was presented: the customized modular rails; manipulator workspace analysis, kinematics, and dynamics; and the system localization and calibration. Field tests and simulations were performed and preliminary results show the feasibility of the concept solution.

Ongoing implementations and future work include:

1. *Software integration*: trajectory generation, control strategy calibration;
2. *Field tests*: field test with the designed robotic system;

Acknowledgements

We gratefully acknowledge the financial support of Energia Sustentável do Brasil and the ANEEL R&D program (contract COPPETEC/UFRJ JIRAU 09/15 6631-0003/2015).

References

Bibuli, M., Caccia, M. and Lapierre, L. (2007). Path-following algorithms and experiments for an autonomous surface vehicle, *IFAC Proceedings Volumes (IFAC-PapersOnline)* **7**(PART 1): 81–86.

Bonacorso, N. G., Goncalves, J. a. a. and Dutra, J. C. (2006). Automation of the processes of surface measurement and of deposition by welding for the recovery of rotors of large-scale hydraulic turbines, *Journal of Materials Processing Technology* **179**(1-3): 231–238.

Camurri, M., Vezzani, R. and Cucchiara, R. (2014). 3d hough transform for sphere recognition on point clouds, *Machine Vision and Applications* **25**(7): 1877–1891.

Diankov, R. and Kuffner, J. (2008). Openrave: A planning architecture for autonomous robotics, *Robotics Institute, Pittsburgh, PA, Tech. Rep. CMU-RI-TR-08-34*.

Goldemberg, J. and Lucon, O. (2007). Energia e meio ambiente no brasil, *Estudos Avançados* **21**(59): 7–20.

Gschwandtner, M., Kwitt, R., Uhl, A. and Pree, W. (2011). BlenSor: Blender Sensor Simulation Toolbox Advances in Visual Computing, Vol. 6939 of *Lecture Notes in Computer Science*, Springer Berlin / Heidelberg, Berlin, Heidelberg, chapter 20, pp. 199–208.

Hazel, B., Côté, J., Laroche, Y. and Mongenot, P. (2012). Field repair and construction of large hydropower equipment with a portable robot, *Journal of Field Robotics* **29**(1): 102–122.

Hourtash, A. (2005). The kinematic hessian and higher derivatives, *Computational Intelligence in Robotics and Automation, 2005. CIRA 2005. Proceedings. 2005 IEEE International Symposium on*, IEEE, pp. 169–174.

Krella, A. K. (2011). The new parameter to assess cavitation erosion resistance of hard pvd coatings, *Engineering Failure Analysis* **18**(3): 855–867.

Li, C. and Wang, Y. (2002). Effect of particle state on the adhesive strength of hvof sprayed metallic coating, *Journal of thermal spray technology* **11**(4): 523–529.

Rusinkiewicz, S. and Levoy, M. (2001). Efficient variants of the ICP algorithm, *Proceedings of International Conference on 3-D Digital Imaging and Modeling, 3DIM* **2001-January**: 145–152.

Sciavicco, L. and Siciliano, B. (2000). Differential kinematics and statics, *Modelling and Control of Robot Manipulators*, Springer, pp. 79–129.

Tombari, F. and Di Stefano, L. (2010). Object recognition in 3D scenes with occlusions and clutter by Hough voting, *Proceedings - 4th Pacific-Rim Symposium on Image and Video Technology, PSIVT 2010* pp. 349–355.